

## SYSTEMIC REVIEW



# System for maintaining optimal temperature modes of solar power plants

S S Dorzhiev<sup>1\*</sup>, V A Majorov<sup>1</sup>, E G Bazarova<sup>1</sup>, Paramvir Singh Ahluwalia<sup>2</sup>,  
M I Rosenblum<sup>1</sup>

<sup>1</sup> Federal State Budgetary Scientific Institution "Federal Scientific Agroengineering Center "VIM", 1st Institut'sky proezd, 5, 109428, Moscow, Russia. Tel.: +8-925-346-3747  
<sup>2</sup> Vertex Industrial Engineering LLP, Delhi, India

 OPEN ACCESS

**Received:** 18.12.2020

**Accepted:** 13.03.2021

**Published:** 30.03.2021

**Citation:** Dorzhiev SS, Majorov VA, Bazarova EG, Ahluwalia PS, Rosenblum MI (2021) System for maintaining optimal temperature modes of solar power plants. Indian Journal of Science and Technology 14(9): 826-842. <https://doi.org/10.17485/IJST/v14i9.2184>

## \* Corresponding author.

Tel: +8-925-346-3747  
[Dss.61@mail.ru](mailto:Dss.61@mail.ru)

**Funding:** None

**Competing Interests:** None

**Copyright:** © 2021 Dorzhiev et al. This is an open access article distributed under the terms of the [Creative Commons Attribution License](https://creativecommons.org/licenses/by/4.0/), which permits unrestricted use, distribution, and reproduction in any medium, provided the original author and source are credited.

Published By Indian Society for Education and Environment ([iSee](https://www.indjst.org/))

## ISSN

Print: 0974-6846

Electronic: 0974-5645

## Abstract

**Objectives:** To ensure efficient operation of solar modules and temperature mode in accordance with standard test conditions range within 20-30°C. **Methods:** A mathematical model was developed using the laws of photoelectricity, heat and mass transfer, which provides improvement in the efficiency of solar power plants. Findings: This study presents the theoretical analysis of different embodiment for systems of solar modules using physical and mathematical models. The main design and functional characteristics of solar modules were calculated: temperature and efficiency depending on internal parameters and ambient environment. Dependence between temperature and efficiency of solar modules for different values of air temperature, emissivity factor of solar cells, and efficiency of solar power plants, were determined and presented in the form of diagrams. It was found that solar modules have the highest heating temperature at solar irradiance of  $E_c=1200 \text{ W/m}^2$ , air temperature of  $T_a=50^\circ\text{C}$ , and that the solar modules have the lowest heating temperature at  $T_a=30^\circ\text{C}$  and  $\varepsilon=0.8$ , with a decrease in the heating temperature from 111 to 38°C, the efficiency decreases at an air temperature of 50°C and at the emissivity factor of  $\varepsilon=0.8$  and 0.3 and makes from 4.2 to 10.3%. The dependences were calculated for different latitudes  $\varphi$ : 56°(Moscow), 45°(Krasnodar), 35.5°(Eslamshahr, Iran), 31.6°(Béchar, Algeria), 13.1°(Chennai, India). Solar modules with cooling devices were installed in the Istra district of the Moscow region and bench tests, to specific calculated parameters, were carried out under full-scale conditions. **Conclusions:** It was found that the efficiency of solar panels increased significantly due to the use of systems with heat-exchange tubes, and the losses, when using an anti-gravity heat exchanger for cooling photovoltaic cells, reduced by 6-7 times. **Novelty:** Usage of an anti-gravity heat exchanger to cool the photovoltaic cells, to maintain the optimal operating temperature prevent electrical distortion due to extreme temperatures.

**Keywords:** Solar panels; air temperature; cooling; emissivity factor; solar irradiance; anti-gravity tubes; temperature loads; performance improvement

## 1 Introduction

Due to the growing environmental crisis and to ensure the energy security of countries, over the past 15-20 years, an almost explosive growth in the use of renewable energy sources has been observed across the globe (RES)<sup>(1)</sup>. Access to reliable and sustainable energy encourages the inflow of investments, including government investments, to develop a wide range of energy converters, converting energy from renewable sources to energy of consumer-oriented formats in order to fully realize the potential of renewable energy sources in a particular country. Renewable energy systems, included in the centralized energy grids of countries, provide up to 25% of power consumption in some of them.

Systems of stand-alone type are most commonly used in agriculture, both in animal breeding<sup>(2)</sup> and plant growing<sup>(3)</sup>.

Currently, the development and creation of thermal and photovoltaic modules is one of the key directions in the development of solar energy<sup>(4-7)</sup>. The main objective of this work is to increase the efficiency of solar power conversion, by reducing the loss of incoming solar power and, as a result, to reduce the cost of the produced energy<sup>(8,9)</sup>. The estimated payback period based on the experimental model of photovoltaic modules with a cooling system on areas of more than 8 square meters is 30-40 percent less in comparison with conventional photovoltaic modules. The proposed installation will increase the efficiency of photovoltaic modules and power generation, as well as increase the service life of photovoltaic modules by cooling with heat pipes.

It is known that only 6 – 20% of solar radiation, incident on a photocell, is used to generate electricity. The rest of the energy, to a greater extent, is spent on heating the photocell, resulting in a significant increase in its surface temperature, which, in turn, has a negative impact on its operation<sup>(10-12)</sup>.

Standard Test Conditions (STC) for solar modules with a capacity of 1 kWp/m<sup>2</sup> are applied for their operating temperature of 25°C.

With solar irradiance of 1000-1200 W/m<sup>2</sup>, the cells heat up to 60-70°C, each losing 0.07-0.09 V. This is the main reason for the reduction in the efficiency of solar modules.

The aim of this work is to develop mathematical models, describing the operation of individual units of the system, to study the thermal behavior of a solar module and a system for maintaining optimal temperature modes of photovoltaic cells to improve the efficiency of solar power plants.

## 2 Materials and Methods

When using solar panels, the main task is to reduce photovoltaic losses during their operation. To maintain the optimal operating temperature of photovoltaic cells and prevent distortion of electrical characteristics induced by extreme temperatures, the provision is made to cool the photovoltaic detector of a solar module due to heat exchange between the substrate of photovoltaic cells and the lower soil horizon using an antigravity heat exchanger. In the process of heat exchange, heat is transferred by a cooling agent from the evaporation zone of the antigravity device down to the condensation zone, where the coolant is condensed due to transferring the latent heat of vaporization to the lower soil horizon at a depth of 3-5 meters, depending on climatic conditions, wherefrom the coolant, in liquid form, rises along the capillary body up to the evaporator. The coolant regeneration process is repeated cyclically. In this case, the coolant parameters are selected in a manner that the boiling point coincides with the lower limit of the range of temperatures optimal for the operation of photovoltaic cells. In addition, the filling depth of the condenser part of the antigravity heat exchanger is chosen in such a way that the soil temperature ensures the coolant cooling to the temperature optimal for the operation of photovoltaic cells, which makes from 30 to 50% of the annual soil heating depth. In the process of the method implementation, the photovoltaic module is cooled to an optimum temperature of 20-30°C. This results to an increase in the solar module efficiency.

### 2.1. Analytical methods for calculating the heating temperature of solar panels without accounting for the atmospheric parameters

The temperature of solar modules (SMs), without accounting for the atmospheric parameters, is determined by heat transfer via radiation. The equilibrium operating temperature of SMs is determined by the equation<sup>(13)</sup>:

$$T_{pa\delta} = \left[ \frac{(a - f_{fill} \cdot \eta) s_{pp} E_c \cos y}{(\epsilon S_{fill} + \epsilon S_{tp}) \sigma} \right]^{1/4} \quad (1)$$

where  $a$  is the integral absorption coefficient of solar radiation (SR) of the surface of solar cells (SCs),

$f_{fill}$  is the filling factor of SCs of the SM panel,

$\eta$  is the actual efficiency of SCs,  $S_{pp}$  is the area of the SM front surface,  
 $E_c$  is the solar constant,  $W/m^2$ ,  
 $\gamma$  is the angle of incidence of solar radiation on the SM,  
 $\epsilon$  is the SR absorption coefficient of the SM front surface,  
 $\epsilon'$  is the SR absorption coefficient of the SM dark surface,  
 $S_{dp}$  is the area of the SM dark surface,  
 $\sigma$  is the Stefan-Boltzmann constant ( $\sigma=5.67 \cdot 10^{-8}$ ,  $W/m^2K^4$ ).

Heat removal from solar modules occurs due to heat exchange with the ambient air through convection and radiation. Various systems of forced cooling of photovoltaic detectors can be used to increase the efficiency of solar panels (SMs)<sup>(14-16)</sup>.

For applications of air-cooling systems, the thermal behavior of a solar module with solar cells is studied when cooled by atmospheric air and via natural heat exchange with the environment. Heat transfer between the environment and the radiator occurs according to Newton's law<sup>(17)</sup>.

$$W_{mn} = \eta_{opt} E_c F_{ap} \tag{2}$$

Electric power:

$$W_{el} = \eta_{se} \eta_{onn} W_{pp} \tag{3}$$

where  $\eta_{se}$  is the efficiency of solar cells, p.u.,  $\eta_{opt}$  is the optical efficiency of SMs.

The efficiency of solar cells depends on temperature<sup>(18)</sup>:

$$\eta = \eta_0 [1 - k(T_f - T_0)] \tag{4}$$

where  $\eta_0$  is the efficiency of solar cells at standard temperature of  $T_0=298$  K,  $T$  is the temperature of solar cells, K;  $k$  is the temperature coefficient ( $k$  is less than 0.003).

Heat losses to the environment:

- Induced by convection:

$$W_{conv} = \alpha (t_c - t_a) F \tag{5}$$

where  $\alpha$  is the heat transfer coefficient, determined according to the McAdams formula  $W/(m^2K)$ ,  $\alpha = 5.7+3.8V$ ,  $t_c$  is the mean temperature of the receiver wall, determined by iteration<sup>(19)</sup>;  $F$  is the module area,  $m^2$ ;  $V$  is the airflow rate,  $m/s$ .

- Induced by radiation:

$$W_{rad} = \epsilon \sigma (T_c^4 - T_a^4) F \tag{6}$$

where  $\epsilon$  is the emissivity factor;  $\sigma$  is the Stefan-Boltzmann constant,  $W/m^2 K^4$ ;  $T$  is the absolute temperature, K.  $T_c$  and  $T_a$  are absolute temperatures of the radiating surface and the environment.

The flux of solar radiation, entering the solar panel surface, is spent on photovoltaic conversion, heating the module, transferring heat to the environment and is determined by the formula:

$$W_{pp} = W_{el} + W_{conv} + W_{rad} \tag{7}$$

Substituting the values of  $W_{el}$ ,  $W_{conv}$ ,  $W_{rad}$ , expressed by the set of equations (2) - (6), into equation (7), we obtain a complex dependence of the heating temperature of SMs on the environmental parameters: solar irradiance  $E_c$ , air temperature  $T_a$ , wind speed  $V$  and the SM parameters: the emissivity factor  $\epsilon$ , the efficiency of solar cells  $\eta_{se}$ , the optical efficiency  $\eta_{opt}$ .

The solution of the set of equations was reduced to determining the functional dependence of each component of equation (6) on temperature under the boundary condition:

$$\frac{W_{pp}}{\sum W} = 1 \tag{8}$$

Where  $\sum W = W_{el} + W_{conv} + W_{rad}$

## 2.2 Analytical methods for calculating the operation of various solar panels

The calculation of the operation of SMs with accurate tracking is based on the known dependence of the hour angle  $\omega$  of the Sun's motion (from sunrise to sunset), on the declination angle  $\delta$  and the location latitude  $\varphi$ :

$$\cos \omega_{\mu} = \tan \delta \tan \varphi \tag{9}$$

The operation time of SMs with tracking,  $t_{tr}$ , h, is determined according to the expression:

$$t_{tr} = \frac{\arccos(\tan \delta \tan \varphi)}{a} \tag{10}$$

where  $a=0.2618$  rad/h ( $15^{\circ}$ /h) is the Sun's rate of motion (the Earth's rotation rate).

The calculation of the operation time of (planar) stationary SMs is based on the dependence of the hour angle of the SM operation  $\omega$  on the declination angle  $\delta$  and the difference  $\Delta s$  between the latitude  $\varphi$  and the angle of the SM inclination to the horizon  $s$ ,  $\Delta s = \varphi - s$ .

In the summertime  $\sin \omega$  corresponds to the obtained expression:

$$\sin \omega_H = \tan \delta \tan \Delta s \tag{11}$$

The declination angle  $\delta$  depends on the annual angle  $w$  and corresponds to the expression:

$$\delta = \delta_c \cos \omega \tag{12}$$

where  $\delta$  is the angle between the Earth's rotation axis and the plane of its motion around the Sun ( $\delta=23.5^{\circ}$ ). The declination  $\delta$  can also be determined using the approximate formula by Cooper.

Expressions obtained:

The operation time of (planar) stationary SMs in summertime:

$$t_{n\pi} = \frac{\pi - \arcsin \omega \pi}{a} \tag{13}$$

The operation time of (planar) stationary SMs in wintertime:

$$t_n = \frac{\arccos(\tan \delta \tan \varphi)}{a} \tag{14}$$

The angle of the Sun inclination during the day to the perpendicular to the SR input surface of a planar SM  $-j$ :

$$\cos j = \frac{\sin \delta}{\tan \tilde{a}} \tag{15}$$

where in summer time  $\pi/2 \leq \tilde{a} \leq \delta$ ; in wintertime  $\omega \leq \tilde{a} \leq \delta$ .

Daily average  $\cos j_{cp}$ :

$$\cos j_{cp} = \frac{\int_{\delta}^j \cos j dj}{\Delta j} \tag{16}$$

For a planar SM:

$$\cos j_{cp} = \frac{\sin \arccos \frac{\sin \delta}{\tan \omega_H} - \sin \delta}{\arccos \frac{\sin \delta}{\tan \omega_H} - \delta} \tag{17}$$

Substituting the values of  $\eta_{opt}$  - optical efficiency, p.u.,  $\eta_{fm}$  - FM efficiency, p.u.,  $t_{sm}$  - SM operation time, h,  $S_{sm}$  - SM area,  $m^2$ ,  $Q_{sm}$  - the SM energy output results in the following expression,  $W \bullet h$ :

$$Q_{sm} = E_{st} t_{sm} S_{sm} \cos j_{cp} \eta_{opt} \eta_{fm} \tag{18}$$

### 2.3 Systems of solar panels with antigravity heat exchangers

To maintain the optimal operating temperature of SMs, including solar cells cooling, it is possible to efficiently use of a system that removes thermal energy from heated solar cells by antigravity heat exchangers into the lower soil horizon to a depth equal to 30 to 50% of the annual soil heating depth<sup>(20,21)</sup>.

The considered physical-mathematical model of the solar photovoltaic system consists of two close-fitting plates of solar cells and a substrate, attached to the evaporative part of an antigravity heat exchanger with different temperatures with the boundary conditions of type IV<sup>(22)</sup>. According to these conditions, at the boundary between these plates, the temperature is set equal to:

$$T = T_M + \frac{(T_{se} - T_M)m}{m + 1} \tag{19}$$

where T is the initial temperature of a metal plate,  $T_{se}$  is the initial temperature of silicon solar cells.

The coefficient m is determined by the formula;

$$m = \sqrt{\frac{\lambda_{se} c_{se} \rho_{se}}{\lambda_M c_M \rho_M}} \tag{20}$$

where  $\lambda$  is the thermal conductivity, c is the heat capacity,  $\rho$  is the density, respectively, of silicon solar cells and a metal plate.

$$k_{se} = 1 - 0.0025 (T_{st} - 25) \tag{21}$$

$$\eta_{sm} = \eta_0 k_{se} \tag{22}$$

where  $\eta_0$  is the initial efficiency of solar cells.

## 3 Results and Discussion

### 3.1 Calculation of the heating temperature of solar panels without accounting for the atmospheric parameters

Based on equation 1, the dependences of the heating temperature of SMs, without accounting for the atmospheric parameters, on solar irradiance, at various values of the integral absorption coefficient of SR a of the surface of solar cells, as well as the dependences of the heating temperature of SMs on the absorption coefficient  $a=\epsilon$  at various values of solar irradiance  $E_c$  were determined and presented in the form of diagrams in [Figures 1, 2, 3, 4 and 5].

Based on equation (1), the dependences of the heating temperature of SMs in a non-atmospheric environment on solar irradiance were calculated at various values of the integral absorption coefficient of SR a of the surface of solar cells, with the results presented in [Figure 1].

The dependences of the heating temperature of SMs on solar irradiance at various values of  $\epsilon$  - the SR absorption coefficient of the front surface of SMs are shown in [Figure 2].

The dependences of the heating temperature of SMs on the absorption coefficient  $a=\epsilon$  at various values of solar irradiance  $E_c$  are shown in [Figure 3].

The dependences of the heating temperature on the SR absorption coefficient of the front surface of SMs  $\epsilon$  at a constant value of  $a=0.8$  at various values of solar irradiance  $E_c$  are shown in [Figure 4].

The dependences of the heating temperature on solar irradiance  $E_c$  at various values of the SR absorption coefficient of the dark surface of SMs  $\epsilon'$  at a constant value of  $a=\epsilon=0.8$  are shown in [Figure 5].

The dependences of the efficiency of solar cells on the heating temperature of SMs without accounting for the atmosphere on the efficiency of solar cells at various values of solar irradiance  $E_c$  at the SR absorption coefficient of the dark surface of SMs  $\epsilon'=0.1$  at a constant value of  $a=\epsilon=0.8$  are shown in [Figure 6].

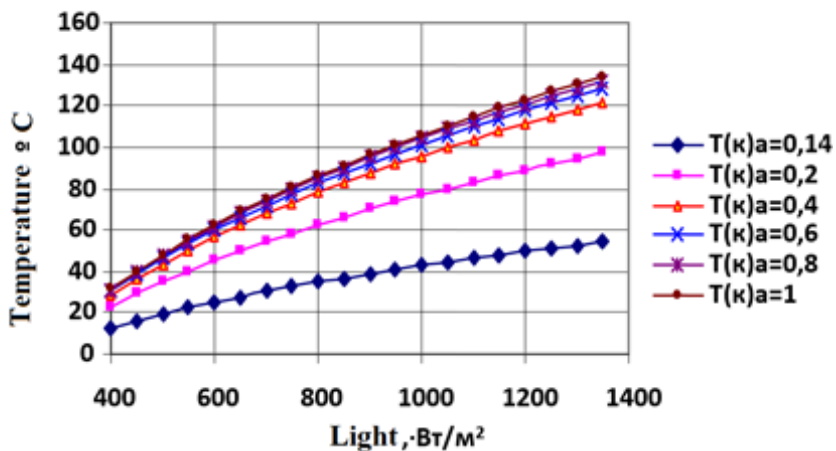


Fig 1. Dependence of the heating temperature of SMs without accounting for the atmosphere on solar irradiance at various values of the integral absorption coefficient of SR  $a$  of the surface of solar cells

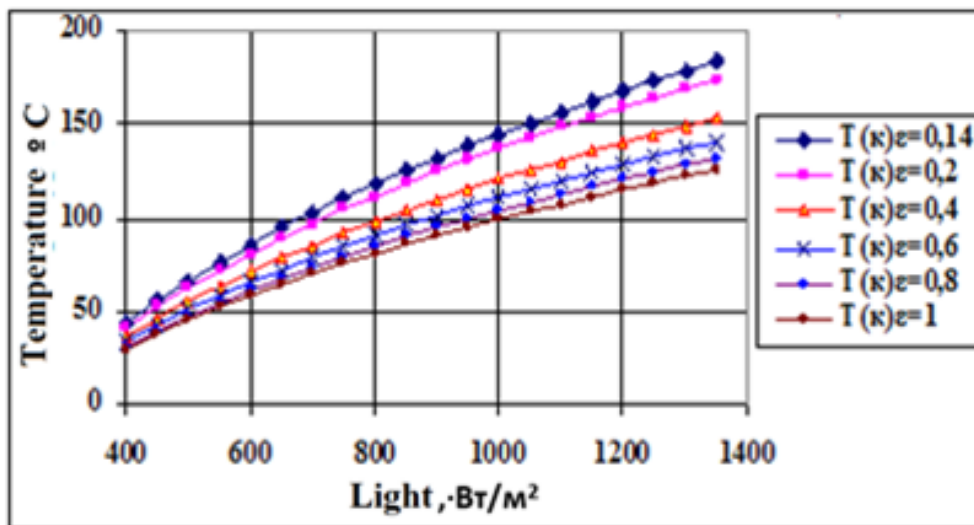


Fig 2. Dependence of the heating temperature of SMs without accounting for the atmosphere on solar irradiance at various values of the SR absorption coefficient of the front surface of SMs  $\epsilon$

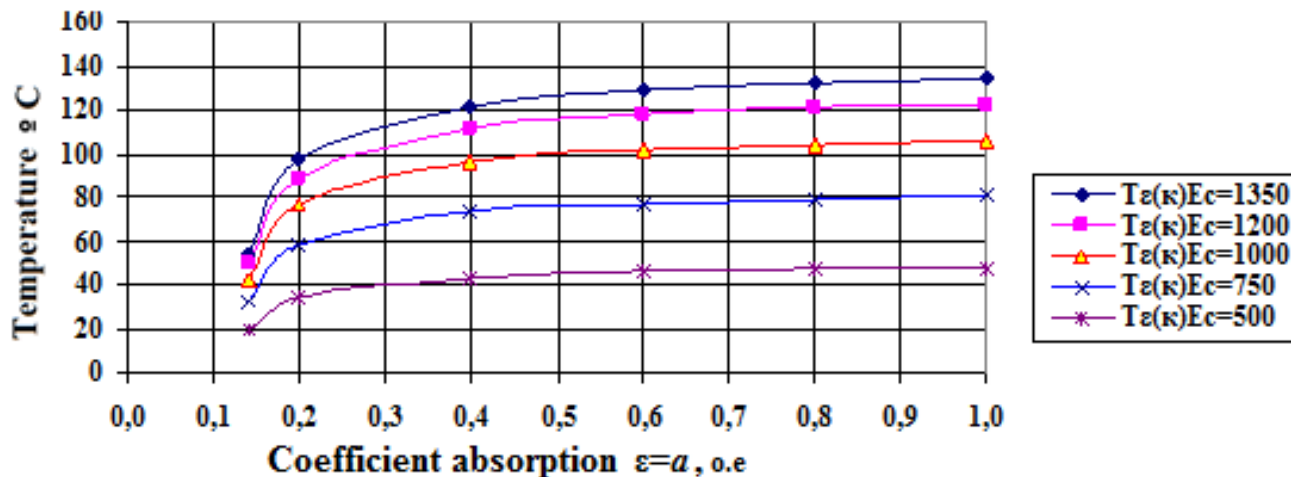


Fig 3. Dependence of the heating temperature of SMs without accounting for the atmosphere on the absorption coefficient  $a=\varepsilon$  at various values of solar irradiance  $E_c$

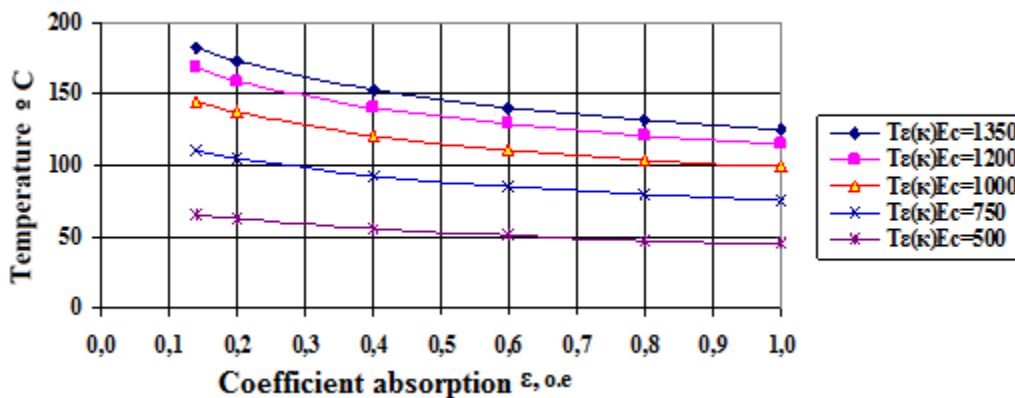


Fig 4. Dependence of the heating temperature of SMs without accounting for the atmosphere on the SR absorption coefficient of the front surface of SMs  $\varepsilon$  at a constant value of  $a = 0.8$  at various values of solar irradiance  $E_c$

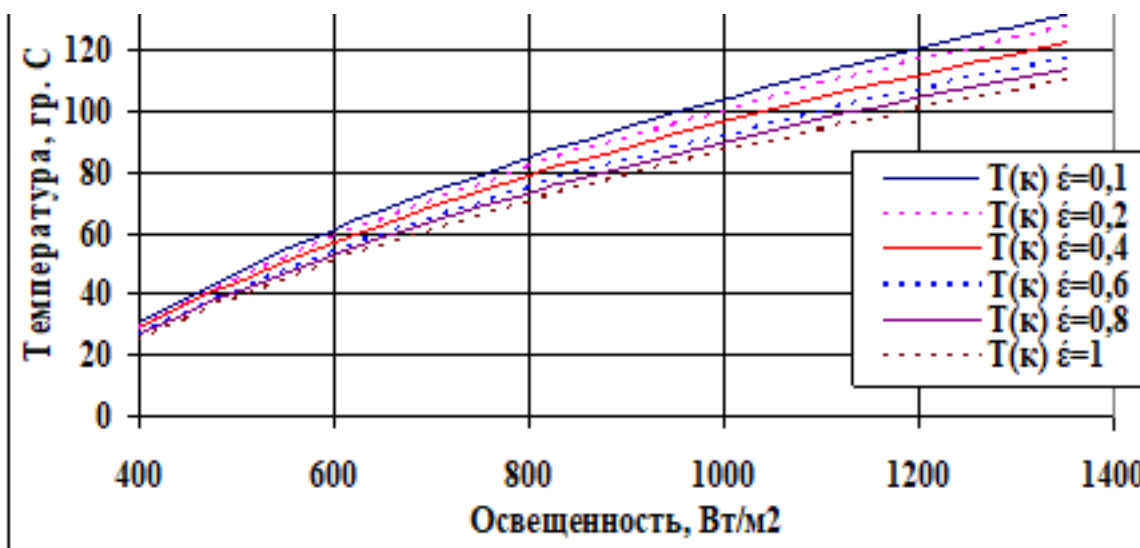


Fig 5. Dependences of the heating temperature of SMs without accounting for the atmosphere on solar irradiance  $E_c$  at various values of the SR absorption coefficient of the dark surface of SMs  $\tilde{\epsilon}$  at a constant value of  $a=\epsilon=0.8$

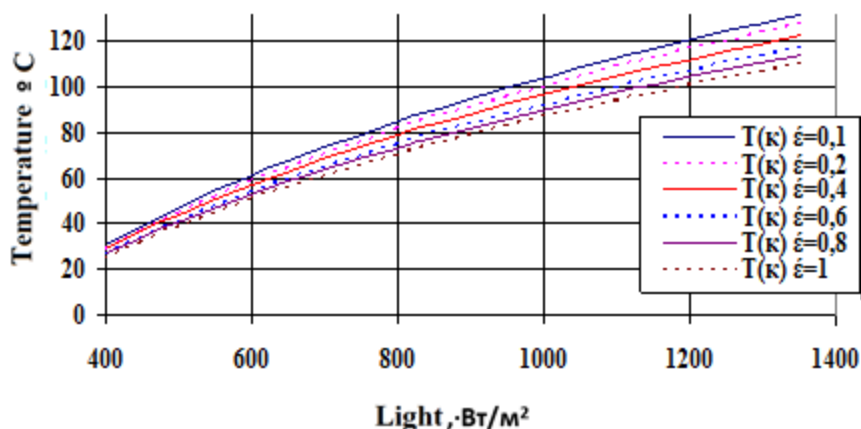


Fig 6. Dependences of the heating temperature of SMs without accounting for the atmosphere on the efficiency of solar cells at various values of solar irradiance  $E_c$  at the SR absorption coefficient of the dark surface of SMs  $\epsilon=0.1$  at a constant value of  $a=\epsilon=0.8$

### 3.2 Calculation of the heating temperature of solar panels taking into account the atmospheric parameters

Southern latitudes are characterized by solar irradiance  $E_c \sim 1200 \text{ W/m}^2$  and summer air temperatures from 30 to 50°C.

Based on equations (1) - (8), the dependences of the heating temperature of solar panels on solar irradiance, on the wind speed, at an air temperature of 30 and 50°C, at the emissivity factor of  $\epsilon=0.8$ , wind speed of  $v=0$  and 3 m/s, were calculated under various operating conditions, with the results presented in [Figure 7].

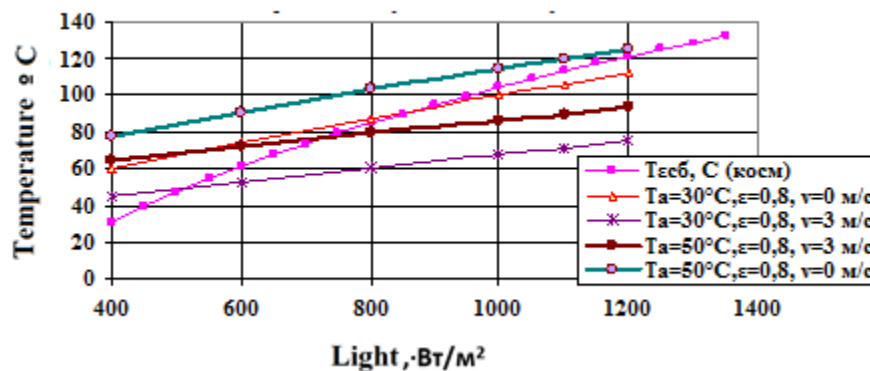


Fig 7. Dependences of the heating temperature of solar panels on solar irradiance under various operating conditions

The presented diagram shows that the heating temperature of solar panels increases with an increase in solar irradiance  $E_c$ , air temperature  $T_a$  and with a decrease in wind speed  $v$ .

The highest heating temperature of solar panels is observed at solar irradiance of  $E_c=1200 \text{ W/m}^2$ , air temperature of  $T_a=50^\circ\text{C}$  and wind speed of  $v=0$ , which exceeds the heating temperature in space.

The calculated dependences of the heating temperature of solar panels on the wind speed, at an air temperature of 20 and 30°C, at the emissivity factor of  $\epsilon=0.8$  and 0.5 and solar irradiance of  $E_c \sim 1000 \text{ W/m}^2$  are presented in [Figure 8].

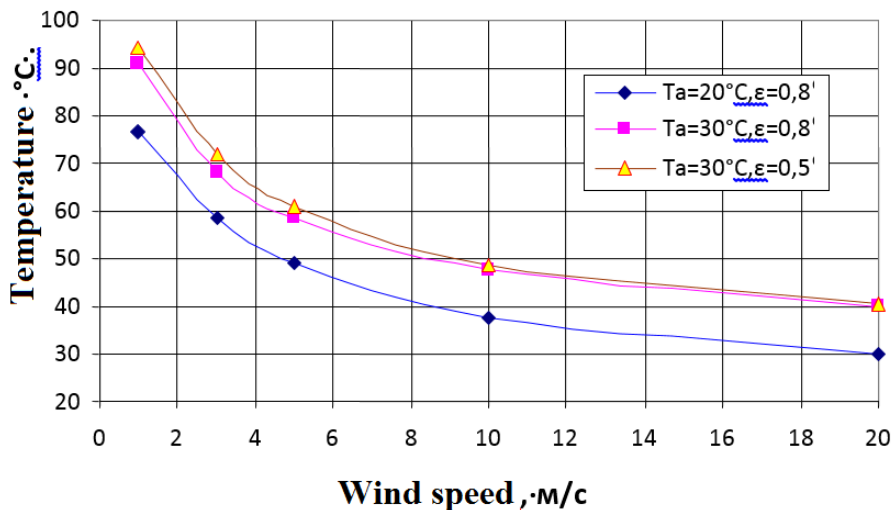


Fig 8. Dependences of the heating temperature of solar panels on the wind speed, at an air temperature of 20 and 30°C, at the emissivity factor of ε=0.8 and 0.5 and solar irradiance of  $E_c \sim 1000 \text{ W/m}^2$

The presented diagram shows that the lowest heating temperature of solar panels is observed at  $T_a=20^\circ\text{C}$  and  $\epsilon=0.8$  and with a decrease in the heating temperature from 78 to 30°C when the airflow rate increases from 1 to 20 m/s.

The highest heating temperature of solar panels is observed at  $T_a=30^\circ\text{C}$  and  $\epsilon=0.5$  and with a decrease in the heating temperature from 95 to 40°C when the airflow rate increases from 1 to 20 m/s.

Low latitudes are characterized by solar irradiance of  $E_c \sim 1200 \text{ W/m}^2$  and summer air temperatures from 30 to 50°C.

The calculated dependences of the heating temperature of solar panels on the wind speed, at an air temperature of 30 and 50°C, at the emissivity factor of ε=0.8 and 0.3 and solar irradiance of  $E_c \sim 1200 \text{ W/m}^2$  are presented in [Figure 9].

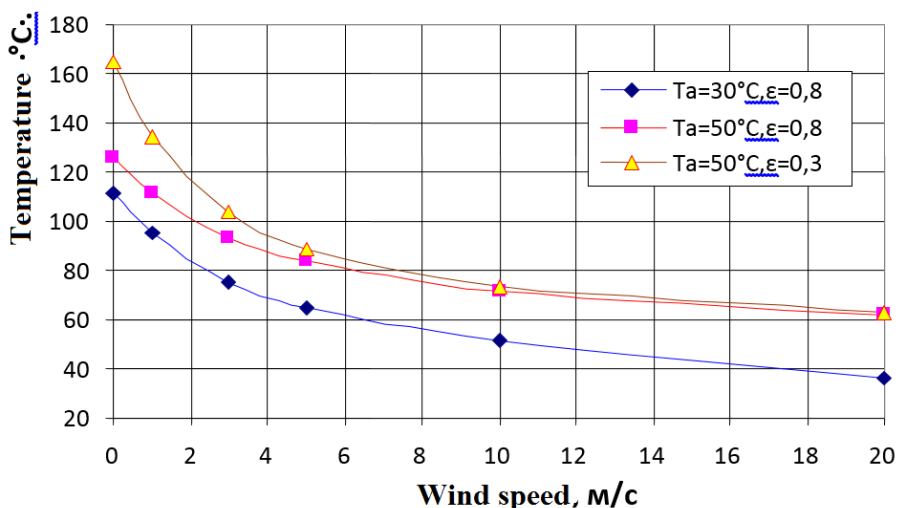


Fig 9. Dependence of the heating temperature of solar panels on the wind speed, at an air temperature of 30 and 50°C, at the emissivity factor of ε=0.8 and 0.3 and solar irradiance of  $E_c \sim 1200 \text{ W/m}^2$

The presented diagram shows that the lowest heating temperature of solar panels is observed at  $T_a=30^\circ\text{C}$  and  $\epsilon=0.8$  and with a decrease in the heating temperature from 111 to 38°C when the airflow rate increases from 0 to 20 m/s.

The highest heating temperature of solar panels is observed at  $T_a=50^\circ\text{C}$  and  $\epsilon=0.3$  and with a decrease in the heating temperature from 164 to 60°C when the airflow rate increases from 0 to 20 m/s.

Thus, to reduce the heating temperature of solar panels, it is necessary to increase the emissivity factor as well as to increase the airflow rate using natural conditions or a forced ventilation system.

When using solar panels, the main task is to reduce photovoltaic losses during their operation.

Middle latitudes are characterized by solar irradiance  $E_c \sim 1000 \text{ W/m}^2$  and summer air temperatures from 20 to 30°C.

The calculated dependences of the efficiency of solar panels at  $\eta_c=5\%$ ,  $\eta_o=0.8$  on the wind speed, at an air temperature of 20 and 30°C, at the emissivity factor of  $\epsilon=0.8$  and 0.5 and solar irradiance of  $E_c \sim 1000 \text{ W/m}^2$  are presented in [Figure 10].

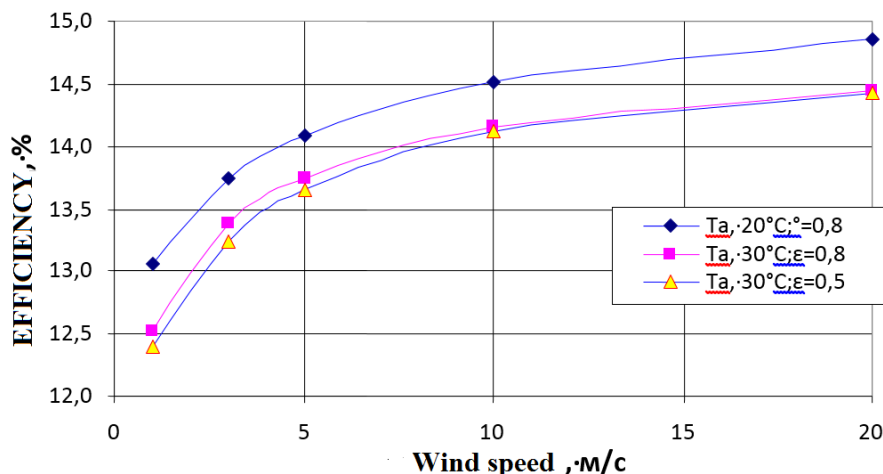


**Fig 10.** Calculated dependence of the efficiency of solar panels on the wind speed, at an air temperature of 20 and 30°C, at the emissivity factor of  $\epsilon=0.8$  and 0.5 and solar irradiance of  $E_c \sim 1000 \text{ W/m}^2$

The presented diagram shows that the lowest heating temperature of solar panels is observed at  $T_a=30^\circ\text{C}$  and  $\epsilon=0.8$  and the efficiency increases from 13 to 14.8% with an increase in the airflow rate from 1 to 20 m/s. The efficiency reduction at the airflow rate of 1 m/s makes 20%.

The highest heating temperature of solar panels is observed at  $T_a=30^\circ\text{C}$  and  $\epsilon=0.5$  and the efficiency increases from 12.4 to 13.9% with an increase in the airflow rate from 1 to 20 m/s. The efficiency reduction at the airflow rate of 1 m/s makes 21%.

The efficiency reduction at the airflow rate of 20 m/s at an air temperature of 20 and 30°C and at the emissivity factor of  $\epsilon=0.8$  and 0.5 ranges from 0.7 to 4.2%.

The calculated dependences of the efficiency of solar panels at  $\eta_c=15\%$ ,  $\eta_o=0.8$  on the wind speed, at an air temperature of 20 and 30°C, at the emissivity factor of  $\epsilon=0.8$  and 0.3 and solar irradiance of  $E_c \sim 1200 \text{ W/m}^2$  are presented in [Figure 11].

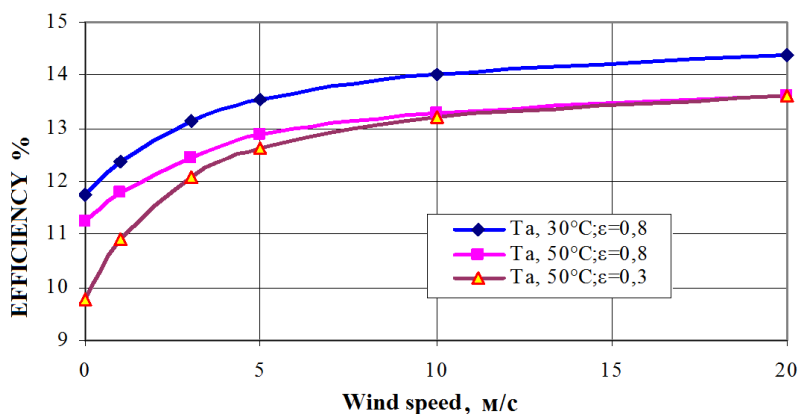


**Fig 11.** Calculated dependences of the efficiency of solar panels on the wind speed, at an air temperature of 30 and 50°C, at the emissivity factor of  $\epsilon=0.8$  and 0.3 and solar irradiance of  $E_c \sim 1200 \text{ W/m}^2$

The presented diagram shows that the lowest heating temperature of solar panels is observed at  $T_a=30^\circ\text{C}$  and  $\varepsilon=0.8$  and the efficiency increases from 11.8 to 14.4% with an increase in the airflow rate from 0 to 20 m/s. The efficiency reduction at the airflow rate of 0 m/s makes 27%.

The highest heating temperature of solar panels is observed at  $T_a=50^\circ\text{C}$  and  $\varepsilon=0.3$  and the efficiency increases from 9.8 to 13.5% with an increase in the airflow rate from 0 to 20 m/s. The efficiency reduction at the airflow rate of 0 m/s makes 53%.

The efficiency reduction at the airflow rate of 20 m/s at an air temperature of 50 and  $50^\circ\text{C}$  and at the emissivity factor of  $\varepsilon=0.8$  and 0.3 ranges from 4.2 to 10.3%.

Thus, to increase the efficiency of solar panels, it is necessary to increase the emissivity factor as well as to increase the airflow rate using natural conditions or a forced ventilation system.

### 3.3 Calculation of the operation of various security systems

Southern latitudes are characterized by solar irradiance  $E_c \sim 1200 \text{ W/m}^2$  and summer air temperatures from 30 to  $50^\circ\text{C}$ . The dependences of power generated for stationary solar panels with an area of  $10 \text{ m}^2$  and solar panels with accurate tracking on the time of the year (June-December) for different latitudes  $\phi$ :  $56^\circ$ (Moscow),  $45^\circ$ (Krasnodar),  $35.5^\circ$ (Eslamshahr, Iran),  $31.6^\circ$ (Béchar, Algeria),  $13.1^\circ$ (Chennai, India) at  $T_a= 30^\circ\text{C}$ ,  $\varepsilon=0.8$ ,  $v=3 \text{ m/s}$ , with the initial efficiency of solar cells  $\eta_{oc}=15\%$ ,  $\eta_o=0.9$ ,  $E_c=1100\text{W/m}^2$ , and the efficiency of solar cells  $\eta_c=12.1\%$  at the heating temperature of  $T_c=72^\circ\text{C}$ , calculated under completely cloudless weather conditions, are presented in [Figure 12].

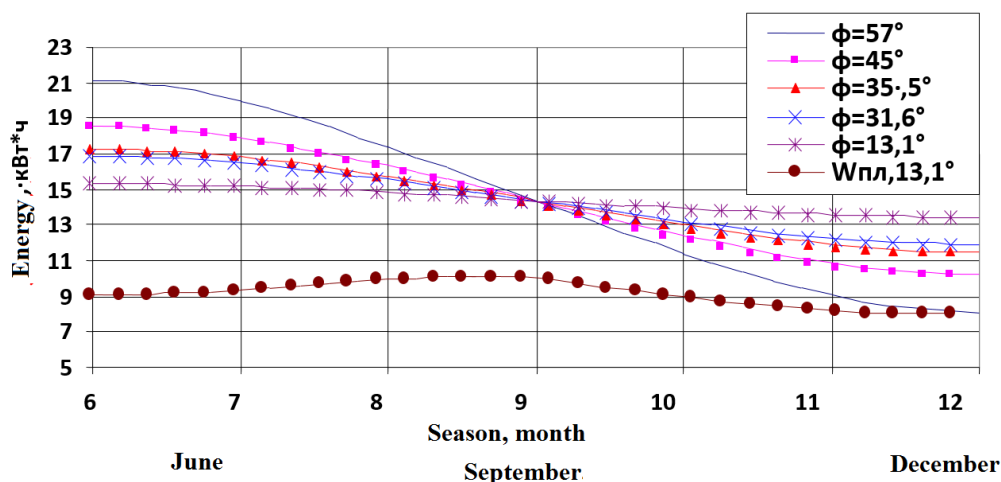


Fig 12. Dependences of energy generated for stationary solar panels with an area of  $10 \text{ m}^2$  and solar panels with accurate tracking on the time of the year (June – December) for different latitudes under completely cloudless weather conditions

As is seen from the diagram, solar panels with accurate tracking generates 1.5-1.7 times more energy per year than stationary planar solar panels (lower curve).

Based on the NASA tabular data on the horizontal illumination of the Earth’s surface at latitudes  $56^\circ$  (Moscow),  $40.4^\circ$  (Madrid - continental region),  $23.1^\circ$  (Havana - coastal region), the calculation of the decrease in daylight illumination from June to December was performed, with the results presented in [Table 1].

Table 1. Coefficients for the reduction of daylight illumination from June to December

	23.1°tab	40.4°tab	56°tab
6	1.00	1.00	1.00
7	1.00	1.04	1.07
8	1.05	1.15	1.26
9	1.14	1.40	1.78
10	1.32	1.88	2.97
11	1.55	2.44	5.95
12	1.73	2.83	10.90

The greatest decrease in daylight illumination from June to December is observed in northern latitudes (Moscow), the smallest – in southern latitudes in coastal regions (Havana).

Using these coefficients, the dependences of energy generated for stationary solar panels with an area of 10 m<sup>2</sup> and solar panels with accurate tracking on the time of the year (June-December) for different latitudes  $\phi$ : 56° (Moscow), 45° (Krasnodar), 35.5° (Eslamshahr, Iran), 31.6° (Béchar, Algeria), 13.1° (Chennai, India - coastal region) at  $T_a=30^\circ\text{C}$ ,  $\varepsilon=0.8$ ,  $v=3\text{ m/s}$ , with the initial efficiency of solar cells  $\eta_{ose}=15\%$ ,  $\eta_{opt}=0.9$ ,  $E_c=1100\text{ W/m}^2$ , and the efficiency of solar cells  $\eta_{se}=12.1\%$  at a heating temperature of  $T_c=72^\circ\text{C}$ , were (approximately) calculated under completely cloudless weather conditions, with the results presented in [Figure 13].

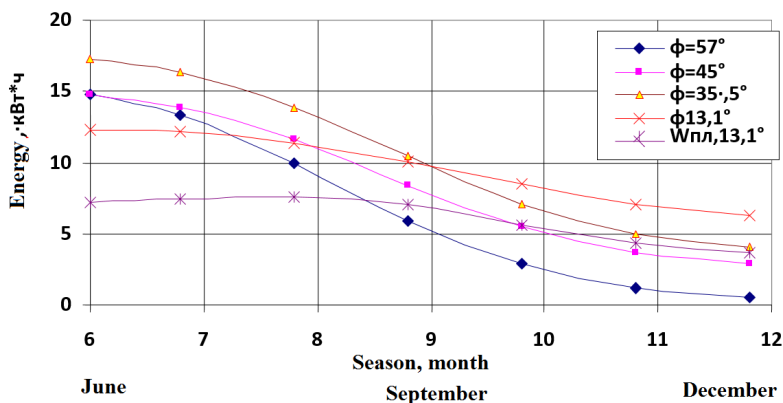


Fig 13. Dependence of energy generated for stationary solar panels with an area of 10 m<sup>2</sup> and solar panels with accurate tracking on the time of the year (June – December) for different latitudes

The presented dependences show that the greatest energy generation is observed in the continental regions of the southern latitudes of 35.5° (Eslamshahr, Iran).

Thus, the above calculation methods allow performing a comparative analysis of energy parameters taking into account the location latitude for the modules and installations being developed.

### 3.4 Systems of solar panels with antigravity heat exchangers

The calculated dependences of the efficiency of solar panels at  $\eta_o=15\%$ ,  $\eta_{opt}=0.8$  on the heating temperature for various substrate materials are presented in Figure 14.

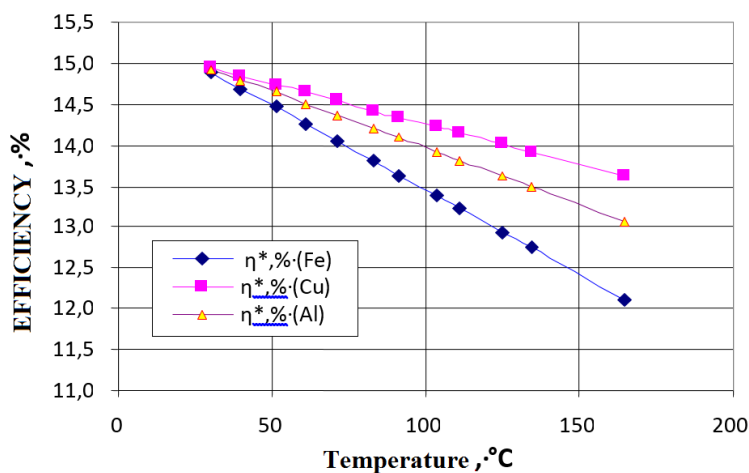


Fig 14. Calculated dependences of the efficiency of solar panels at  $\eta_o=15\%$ ,  $\eta_{opt}=0.8$  on the heating temperature for various substrate materials

The presented diagram shows that a solar panel with a copper substrate has the smallest decrease in the efficiency, from 15 to 13.6%, with an increase in the heating temperature from 30 to 165°C; and a solar panel with a steel substrate has the greatest decrease in the efficiency, from 15 to 12.1%, with an increase in the heating temperature from 30 to 165°C.

In case of such a design of the solar panel, the impact of an air temperature  $T_a$ , the emissivity factor  $\epsilon$ , the airflow rate and solar irradiance  $E_c$  is taken into account.

The calculated dependences of the efficiency of solar panels at  $\eta_o=15\%$ ,  $\eta_{opt}=0.8$  on the wind speed at  $T_a=20^\circ\text{C}$  and  $\epsilon=0.8$ ,  $E_c=1000\text{ W/m}^2$  for different substrate materials are presented in Figure 15.

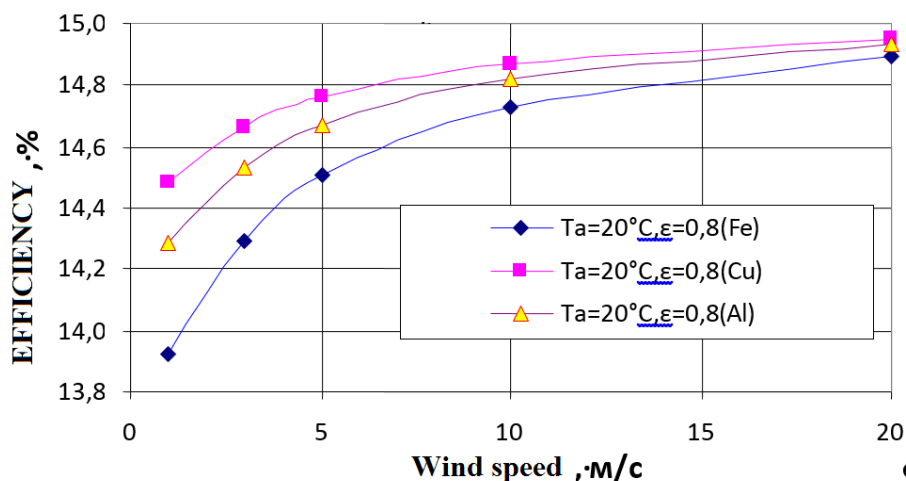


Fig 15. Dependences of the efficiency of solar panels at  $\eta_o=15\%$ ,  $\eta_{opt}=0.8$  on the wind speed at  $T_a=20^\circ\text{C}$  and  $\epsilon=0.8$ ;  $E_c=1000\text{ W/m}^2$  for various substrate materials (Fe, Cu, Al)

A solar panel with a copper substrate has the smallest decrease (3.4%), an increase in the efficiency from 14.5 to 14.9% (2.8%), with an increase in the wind speed from 1 to 20 m/s.

A solar panel with a steel substrate has the greatest decrease (13.6%), an increase in the efficiency from 13.9 to 14.7% (3.4%), with an increase in the wind speed from 1 to 20 m/s.

The calculated dependences of the efficiency of solar panels at  $\eta_o=15\%$ ,  $\eta_{opt}=0.8$  on the wind speed at  $T_a=30^\circ\text{C}$  and  $\epsilon=0.8$ ,  $E_c=1200\text{ W/m}^2$  for various substrate materials are presented in Figure 16.

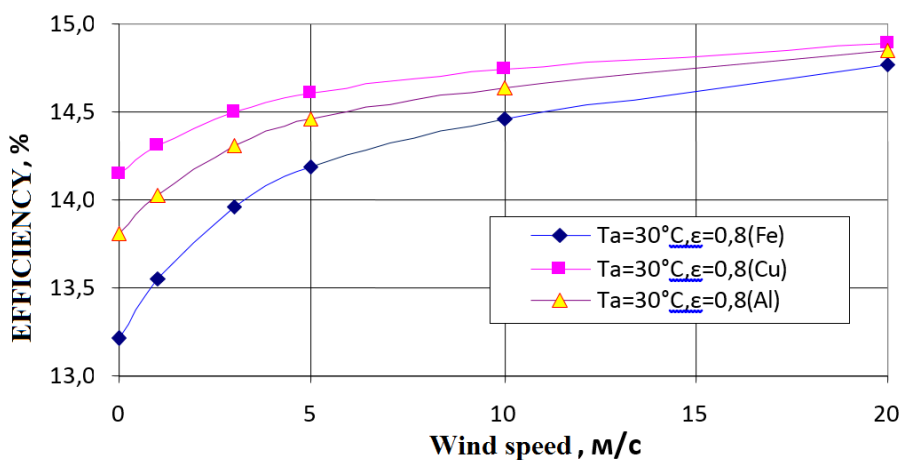


Fig 16. Dependences of the efficiency of solar panels at  $\eta_o=15\%$ ,  $\eta_{opt}=0.8$  on the wind speed at  $T_a=30^\circ\text{C}$  and  $\epsilon=0.8$ ;  $E_c=1200\text{ W/m}^2$  for various substrate materials (Fe, Cu, Al)

The presented diagram shows that a solar panel with a copper substrate has the smallest decrease (6.4%), an increase in the efficiency from 14.2 to 14.8% (5.7%), with an increase in the wind speed from 0 to 20 m/s.

A solar panel with a steel substrate has the greatest decrease (14%), an increase in the efficiency from 13.2 to 14.6% (12.1%), with an increase in the wind speed from 0 to 20 m/s.

Having compared the calculated curves, it can be seen that the loss of systems without heat pipes at a minimum wind speed at  $T_a=50^\circ\text{C}$  and  $\varepsilon=0.8$ ,  $E_c=1200\text{ W/m}^2$  is 34%, and for systems with heat pipes– 5.7%. At  $T_a=30^\circ\text{C}$  and  $\varepsilon=0.8$ ,  $E_c=1000\text{ W/m}^2$ , it makes 20%, and for systems with heat pipes – 2.8%.

Thus, to reduce the heating temperature of solar panels, it is necessary to increase the emissivity factor as well as to increase the airflow rate using natural conditions or a forced ventilation system. The efficiency of solar panels increases significantly due to the use of heat pipe systems.

### 3.5 Experimental module

In order to develop and create new thermal and photovoltaic solar modules with antigravity heat exchange systems, solar modules with cooling devices were developed and bench-tested, to specify the calculated parameters, in full-scale conditions at the wind test center of the FSBSI “Federal Scientific Agroengineering Center “VIM”, in the Istra district of the Moscow region.

[Figure 17] shows the solar module (a) attached to the cooled part of the cooling device with a controlled temperature and mounted on a bench (b) with a biaxial solar tracking system.

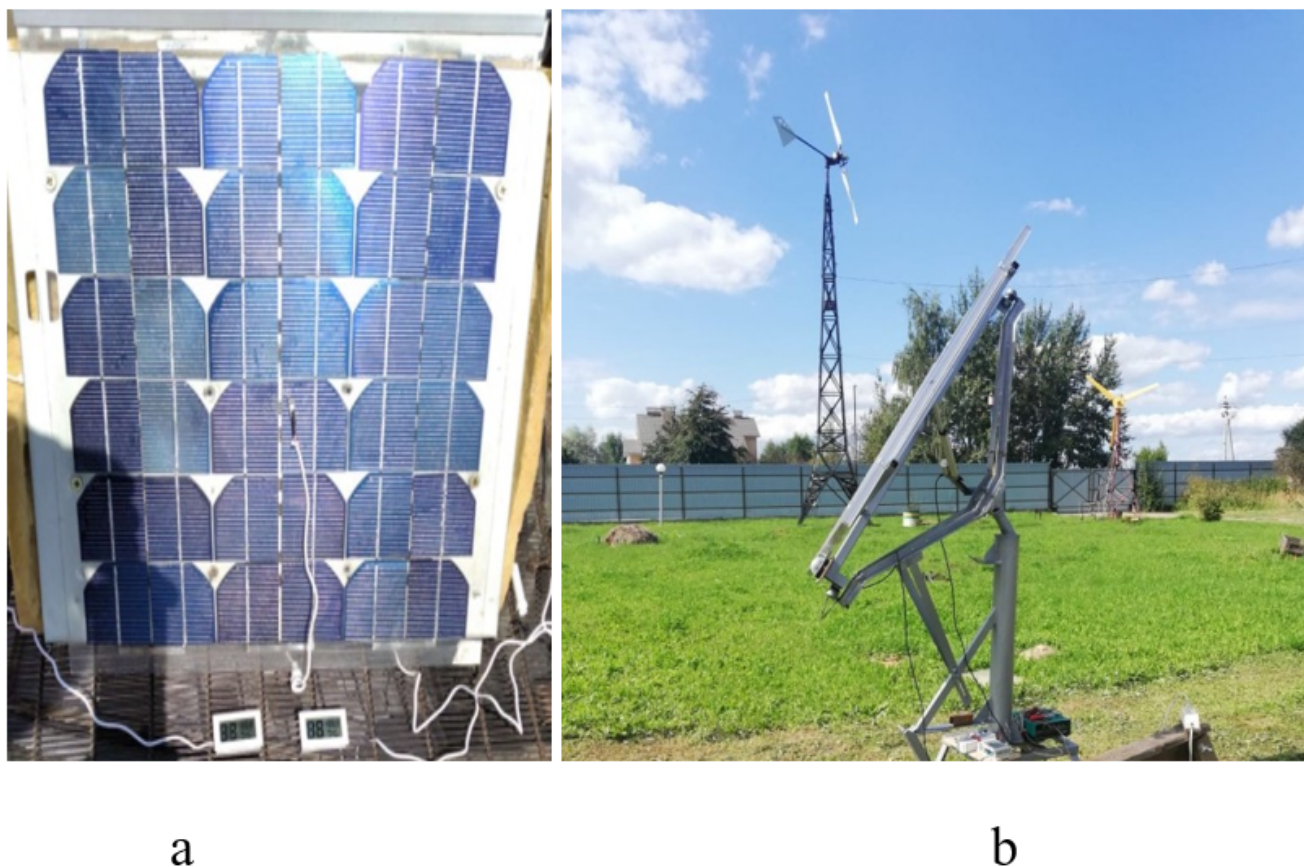


**Fig 17.** Solar module (a) attached to the cooled part of the cooling device with controlled temperature and mounted on a bench (b) with a biaxial solar tracking system

The experimental module operates as follows. Solar radiation, when accurately tracking the Sun, falls perpendicular to the surface of the solar module. The SR receiver is made of a number of solar cells by sequential electrical commutation with a width of  $h_o = \text{cm}$  and a length of  $L = \text{cm}$ . By adjusting the temperature of the cooled part of the cooling device, it is possible to

optimize the heating of solar cells, thereby increasing the module efficiency.

Based on the above calculations, depending on natural conditions - solar radiation output, wind speed, ambient temperature; the module design parameters– optical efficiency, the materials used, it is possible to predict the output parameters (thermal and electrical) and the efficiency of the module as a whole.

## 4 Conclusion

The place of solar power in energy development of the future is determined by the possibilities of industrial use of new physical principles, techniques, materials and designs of solar cells, modules and power plants. The need to develop power supply based on renewable energy sources (RES), especially in rural areas, is now becoming more and more relevant, due to the presence of large territories, power supply of which, via providing therein traditional energy sources, is very challenging, complicated and unprofitable. It is in the latter case that the use of renewable energy sources becomes expedient and frequently cost-effective.

Having studied the impact of temperature on the efficiency of photovoltaic cells, it was revealed that a decrease in the heating temperature of SMs depends on a decrease in the integral absorption coefficient of SR  $\alpha$  of the surface of solar cells, as well as on an increase in the SR absorption coefficient of the front surface of SMs  $\epsilon$  and the SR absorption coefficient of the dark surface of SMs  $\epsilon'$ .

At the same time, the absorption coefficient  $\epsilon$  has a smaller effect on reducing the heating temperature of SMs than the integral absorption coefficient of SR  $\alpha$  of the surface of solar cells, and when the value of the SR absorption coefficient of the dark surface of SMs  $\epsilon'$  changes from 0.1 to 1, the heating temperature of SMs decreases by 18%, while at a similar change in the value of the integral absorption coefficient of SR  $\alpha$  of the surface of solar cells, the heating temperature of SMs increases by 2.5 times.

For applications of air-cooling systems, the thermal behavior of a solar module with solar cells is studied when cooled by atmospheric air and via natural heat exchange with the environment. Based on the developed equations, the dependencies of the heating temperature of SMs on solar irradiance and on temperature and the emissivity factor were calculated under various operating conditions. The presented curves show that the lowest heating temperature of SMs is observed at  $T_a=30^\circ\text{C}$  and  $\epsilon=0.8$  and at a decrease in the heating temperature from 111 to  $38^\circ\text{C}$ . The highest heating temperature of SMs is observed at  $T_a=30^\circ\text{C}$  and  $\epsilon = 0.3$  and at a decrease in the heating temperature from 164 to  $60^\circ\text{C}$ .

Having compared the calculated curves, it was determined that the loss of systems without heat pipes at  $T_a=50^\circ\text{C}$  and  $\epsilon=0.8$ ,  $E_c=1200\text{ W/m}^2$  is 34%, and of systems with heat exchangers – 5.7%. At  $T_a=30^\circ\text{C}$  and  $\epsilon=0.8$ ,  $E_c=1000\text{ W/m}^2$  it makes 20%, and for systems with heat exchangers – 2.8%.

Thus, to reduce the heating temperature of SMs, it is necessary to increase the emissivity factor. The efficiency of SMs increases significantly due to the use of heat pipe systems.

## References

- 1) Solar Power Europe: Global Solar Market Grows over 29% in 2017 with even more to come in 2018. . Available from: <http://www.solarpowereurope.org/media/press-releases/>.
- 2) Palazzi V, Gelati F, Vaglioni U, Alimenti F, Mezzanotte P, Roselli L. Leaf-Compatible Autonomous RFID-Based Wireless Temperature Sensors for Precision Agriculture. *IEEE Topical Conference on Wireless Sensors and Sensor Networks (WiSNet)*. 2019;p. 1–4. Available from: <https://doi.org/10.1109/WISNET.2019.8711808>.
- 3) Hassabou AM, Khan MA. Towards Autonomous Solar Driven Agricultural Greenhouses in Qatar - Integration with Solar Cooling. *7th International Renewable and Sustainable Energy Conference (IRSEC)*. 2019;p. 1–8. Available from: <https://doi.org/10.1109/IRSEC48032.2019.9078285>.
- 4) Sharma SD, Iwata T, Kitano H, Sagara K. Thermal performance of a solar cooker based on an evacuated tube solar collector with a PCM storage unit. *Solar Energy*. 2005;78(3):416–426. Available from: <https://dx.doi.org/10.1016/j.solener.2004.08.001>.
- 5) Avezova NR, Avezov RR, Vokhidov AU, Rakhimov EY, Gaziev UK. Influence of Ambient Temperature, Wind Speed, Emissivity, and Average Working Temperature of Light-Absorbing Heat-Exchange Panels of Flat-Plate Solar Water-Heating Collectors on Their Thermal Losses Through Translucent Coatings. *Applied Solar Energy*. 2019;55(1):30–35. Available from: <https://dx.doi.org/10.3103/s0003701x19010043>.
- 6) Avezov RR, Vokhidov AU, Ibragimov UH, Usmanov AY. Increasing the Convective Heat Transfer Coefficient Inside Heat Removal Channels of Sheet-Piped Light-Absorbing Panels of Flat-Plate Solar Collectors in the Laminar Flow Regime of Heat Transfer Fluid. *Applied Solar Energy*. 2020;56(2):114–117. Available from: <https://dx.doi.org/10.3103/s0003701x20020024>.
- 7) Manxuan X, Llewellyn T, Xingxing Z, Isaac L. A review on recent development of cooling technologies for concentrated photovoltaics systems. *Energies*. 2020;11. Available from: <https://doi.org/10.3390/en11123416>.
- 8) Majorov VA. Principles of Building Systems with Concentrated Solar Energy. *Applied Solar Energy*. 2020;56(3):198–206. Available from: <https://dx.doi.org/10.3103/s0003701x2003007x>.
- 9) Majorov VA. Study of technical and economic indicators of thermal photovoltaic installations based on solar modules with concentrators. *Vestnik VIESH*. 2019;1(34):27–34. Available from: [http://vestnik.viesh.ru/wp-content/uploads/2019/06/ИЭСХ\\_1\\_2019.pdf](http://vestnik.viesh.ru/wp-content/uploads/2019/06/ИЭСХ_1_2019.pdf).
- 10) Farenbrukh A. Solar cells: Theory and experiment. Ergoatomizdat: Moscow. 1987.
- 11) Alsayah AM. Multiple modern methods for improving photovoltaic cell efficiency by cooling: a review. *Journal of Mechanical Engineering Research & Developments*. 2019;42. Available from: <https://doi.org/10.26480/jmerd.04.2019.71.78>.

- 12) Ren X, Li J, Jiao D, Gao D, Pei G. Temperature-dependent performance of amorphous silicon photovoltaic/thermal systems in the long term operation. *Applied Energy*. 2020;275. Available from: <https://dx.doi.org/10.1016/j.apenergy.2020.115156>.
- 13) Rauschenbach G. Reference for the design of solar panels. Energoatomizdat: Moscow. (Russian reference). *Energoatomizdat: Moscow*. 1983.
- 14) Savchenko IG, Smirnova AN, Tarnizhevsky BV. About the temperature regime of photovoltaic generators with solar radiation concentrators with air cooling. *Geliotekhnika*. 1968;4:19–25.
- 15) Piotrowski LJ, Simões MG, Farret FA. Feasibility of water-cooled photovoltaic panels under the efficiency and durability aspects. *Solar Energy*. 2020;207:103–109. Available from: <https://dx.doi.org/10.1016/j.solener.2020.06.087>.
- 16) Suleymanov SX, Gremenok VF, Khoroshko VV, Ivanov VA, Dyskin VG, Djanklich MU, et al. Optical Characteristics of Antireflection Coatings Based on Al<sub>2</sub>O<sub>3</sub>-SiO<sub>2</sub> for Silicon Solar Cells. *Journal of Applied Spectroscopy*. 2020;87(4):720–723. Available from: <https://dx.doi.org/10.1007/s10812-020-01060-9>.
- 17) Lykov AV. Heat conduction theory. Higher school: Moscow. 1967.
- 18) Yu AD, Evdokimov VM. Photovoltaic basics. SSI VIESH: Moscow. 2007.
- 19) Duffie JA, Beckman WA. Solar Engineering of Thermal Processes. and others, editor;New Jersey. John Wiley&Son, Inc.. 2013.
- 20) Koronovsky NV, Yakusheva AF. Basics of geology. and others, editor;Moscow. 1991.
- 21) Dunn PD, Reay DA. Heat pipes. 3rd ed. Oxford. Pergamon press. 2012.
- 22) Pekhovich AI, Zhidkikh VM. Calculations of the thermal regime of solids. *Energy: Leningrad*. 1976.